Strain-Induced Nonanalytic Short-Range Order in the Spin Glass $Cu_{83}Mn_{17}$

H. Reichert, V. N. Bugaev, O. Shchyglo, A. Schöps, Y. Sikula, and H. Dosch
Max-Planck-Institut für Metallforschung, Heisenbergstrasse 1, 70569 Stuttgart, Germany
(Received 13 April 2001; published 15 November 2001)

We present a theoretical and experimental study of the effect of lattice distortions on the short-range order and the energetics of ordering binary alloys. Applying a reciprocal space approach which accounts for the elastic response of the lattice, the diffuse scattering of the model system $Cu_{83}Mn_{17}$ can be explained with only a few physical parameters. The model calculations point to a nonanalytic diffuse intensity at $q = 0$. X-ray scattering experiments are presented providing clear evidence for this phenomenon which carries detailed information on the strain-induced interaction.

DOI: 10.1103/PhysRevLett.87.236105 PACS numbers: 68.35.Gy, 61.66.Dk, 64.60.Cn, 75.50.Lk

The general scientific interest in disordered solid solutions results from the fact that the remaining short-range order (SRO) in such systems gives access to the underlying pair interaction potential V_{mn} of two constituents at a given distance $\vec{r}_m - \vec{r}_n$:

$$V_{mn} = V_{mn}^{AA} + V_{mn}^{BB} - 2V_{mn}^{AB}, \tag{1}$$

which is the fundamental parameter of alloy theory. One experimental and theoretical focus of the past few decades has been on the occupational SRO in binary alloys $A_{1-x}B_x$ governed by the total effective pair interaction (EPI) potential [1–4].

In a real binary alloy, the size mismatch between the constituents plays a crucial role and gives rise to a positional disorder (local lattice distortions) accompanying the occupational disorder. Subsequently, the total EPI is composed of two terms:

$$V_{mn} = V_{mn}^{(\mathrm{ch})} + V_{mn}^{(\mathrm{si})}. \tag{2}$$

with the chemical interaction $V^{(\mathrm{ch})}$ and the strain-induced interaction $V^{(\mathrm{si})}$ originating from the mechanical degrees of freedom [1,5,6]. Both terms in Eq. (2) are equally essential for the energetics of alloys. The anisotropic strain-induced potential is of infinite range (decaying as r^{-2}). Consequently, its proper incorporation into a microscopic description of disordered systems is a challenging problem. Anisotropic strain-induced interactions have been considered by many groups [5–10], experimental evidence has thus far been found only in the small-angle scattering from phase separating systems [11]. In this Letter, we show by theory and experiment that the SRO diffuse scattering intensity in ordering systems exhibits a nonanalytical behavior at $\vec{q} = 0$ and a modulated intensity around it which is intimately related to these anisotropic long-ranged lattice distortions caused by atomic size mismatch.

Diffuse (x-ray or neutron) scattering by structural disorder [12] reads within the concentration wave formalism in the case of small lattice distortions [1,5]:

$$I_D(\vec{q}) = \langle |c_{\vec{q}}|^2 \rangle \Phi_{\vec{q}}^2, \tag{3}$$

with $\Phi_{\vec{q}} = \overline{f}(\vec{Q} \cdot \vec{A}_{\vec{q}}) - (f_A - f_B)$. $c_{\vec{q}}$ denotes the Fourier transform of the occupation number,

$$c_{\vec{q}} = \sum_{\vec{R}} (c_{\vec{R}} - c) e^{-i\vec{q}\vec{R}}, \qquad c_{\vec{R}} = \begin{cases} 1 & B \text{ atom at site } \vec{R} \\ 0 & \text{otherwise.} \end{cases} \tag{4}$$

$\overline{f}(q) = c_A f_A(q) + c_B f_B(q)$ is the average form factor and $\vec{Q} = \vec{G}_{\mathrm{HKL}} + \vec{q}$ the momentum transfer with $\vec{G}_{\mathrm{HKL}}$ defining the reciprocal lattice vectors (H, K, L). The vector $\vec{A}_{\vec{q}}$ is determined by $\vec{u}_{\vec{q}} = \vec{A}_{\vec{q}} c_{\vec{q}}$ assuming a linear relationship between the Fourier coefficients of the distortion field $\{u_{\vec{q}}\}$ and occupation numbers $\{c_{\vec{q}}\}$.

Conventionally, the observed diffuse scattering is analyzed by real space approaches (for a review, see [12]), which are not able to separate $V^{(\mathrm{ch})}$ and $V^{(\mathrm{si})}$. In turn, the so-deduced EPI potential V_{mn} obtained by inverse Monte Carlo (IMC) methods exhibits a long-range tail which requires for its determination a large number of experimentally measured SRO parameters.

In this Letter, a reciprocal space approach is used to analyze the diffuse scattering pattern from ordering alloys, thereby incorporating the long-ranging lattice distortions via the intrinsic elastic response of the system. One merit of this approach is that all long-ranging features in real space (as the aforementioned lattice distortions) are Fourier transformed to the vicinity of the so-called Γ point ($\vec{q} = 0$). We, thus, will focus in this work particularly to this q-space region which is usually not considered in diffuse scattering studies of ordering alloys. For a critical test, we use the spin-glass system $Cu_{83}Mn_{17}$ which exhibits only small lattice distortions (see [13–17]).

Within a microscopic elasticity theory [5], we express $\vec{A}_{\vec{q}}$ via the Fourier coefficients $\hat{G}_{\vec{q}}$ and $\vec{F}_{\vec{q}}$ of the lattice Green function and of the Kanzaki forces, respectively,

$$\vec{A}_{\vec{q}} = \hat{G}_{\vec{q}} \vec{F}_{\vec{q}} \quad \text{with} \quad \hat{G}_{\vec{q}} = \hat{D}_{\vec{q}}^{-1}, \tag{5}$$

where $\hat{D}_{\vec{q}}$ is the dynamic matrix [18]. By this we also reduce the number of free parameters in the problem dramatically in comparison with conventional diffuse scattering methods. Note that $\vec{F}$ acts on nearest neighbors only in contrast to the long-ranged V_{mn} which is commonly used in

IMC parametrization procedures. The matrix elements of $\hat{G}_{\vec{q}}$ are described in terms of the Born–von-Karman constants. The condition of mechanical stability allows one then to calculate the strain-induced part of the interaction potential [5],

$$V^{(\mathrm{si})}(\vec{q}) = -\vec{F}^{+}_{\vec{q}}\hat{D}^{-1}_{\vec{q}}\vec{F}_{\vec{q}} + N^{-1}\sum_{\vec{q}}\vec{F}^{+}_{\vec{q}}\hat{D}^{-1}_{\vec{q}}\vec{F}_{\vec{q}}, \quad (6)$$

satisfying the normalization condition $\sum_{\vec{q}} V^{(\mathrm{si})}_{mn}(\vec{q}) = V^{(\mathrm{si})}_{m=n} = 0$. In this approach, the individual displacements of the different constituents in each coordination shell are projected into displacement parameters of a "grey matrix" where the individual atoms described by f_A, f_B at each lattice site are replaced by the "average" atom $\overline{f}$.

For cubic systems with small distortions (as for Cu-Mn) the three elastic constants together with the concentration dependence of the lattice parameter are already sufficient to allow a parameter-free calculation of $\Phi_{\vec{q}}$ as well as $\langle|c_{\vec{q}}|^2\rangle$ in Eq. (3). A detailed calculation for the system $Cu_{83}Mn_{17}$ shows that the distortions $|\vec{u}|$ exhibit a rather slow decay with distance, illustrating again the difficulties in handling even small distortion systems in real space. The associated strain-induced part of the interaction potential in real space is shown in Fig. 1 together with the EPI as determined independently from conventional neutron scattering data by inverse Monte Carlo methods [13]. Both EPI's exhibit a long-ranged oscillatory tail with an almost perfect coincidence beyond the fourth coordination shell. This implies that, at large distances, the contribution to the energetics of the system is almost completely determined by the elastic response of the system. In turn, the chemical interaction potential $V^{(\mathrm{ch})}$ has a short-range character and can thus be parametrized by a small number of near neighbor interaction parameters. Note here again that the oscillatory tail of the EPI is due to the lattice distortions present in the systems, but not, as assumed hitherto, due to Friedel oscillations [16].

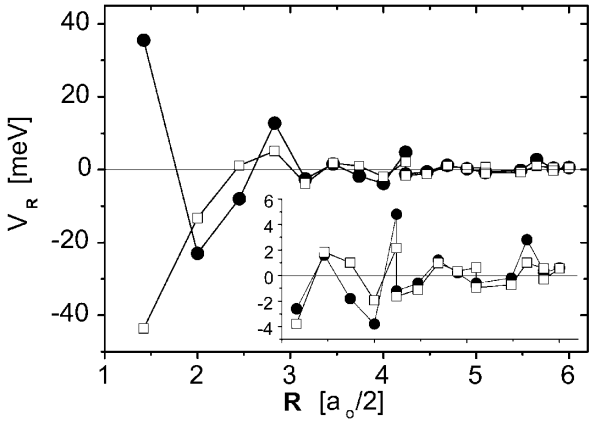

FIG. 1. EPI in real space. The strain-induced contribution $V^{(\mathrm{si})}$ (squares) dominates the total EPI (solid circles) beyond the fourth neighbor shell. The inset magnifies the tail.

In Fig. 2(a), the Fourier components of the chemical and strain-induced parts of the EPI are shown together with the total EPI in various high-symmetry directions. As a general rule, in ordering systems $V^{(\mathrm{ch})}$ and $V^{(\mathrm{si})}$ are large with opposite signs at the Γ point ($\vec{q} = 0$). Consider now the Γ-point behavior more closely: $V^{(\mathrm{si})}(\vec{q} \to 0)$ and, in consequence, $V_{mn}(\vec{q} \to 0)$ have an undefined value which critically depends on the direction from which the Γ point is approached. This nonanalytic character of the total EPI becomes immediately apparent in a polar plot in the (001) plane [see Fig. 2(b)]. Our calculation shows that the nonanalyticity of the EPI at the Γ point is accompanied by a periodic azimuthal variation of the EPI in a wide vicinity around the origin of reciprocal space. This character of the EPI in reciprocal space is generic for all systems exhibiting anisotropic elastic properties and atomic size mismatch [1].

These strain effects have direct implications for the SRO diffuse scattering in the $Cu_{83}Mn_{17}$ system. Figure 3 shows the diffuse scattering intensity in the (001) plane as calculated using Eq. (3), where we have used the concentration waves $\langle|c_{\vec{q}}|^2\rangle$ deduced from the total EPI by means of the ring approximation [19]. One finds the well-known diffuse

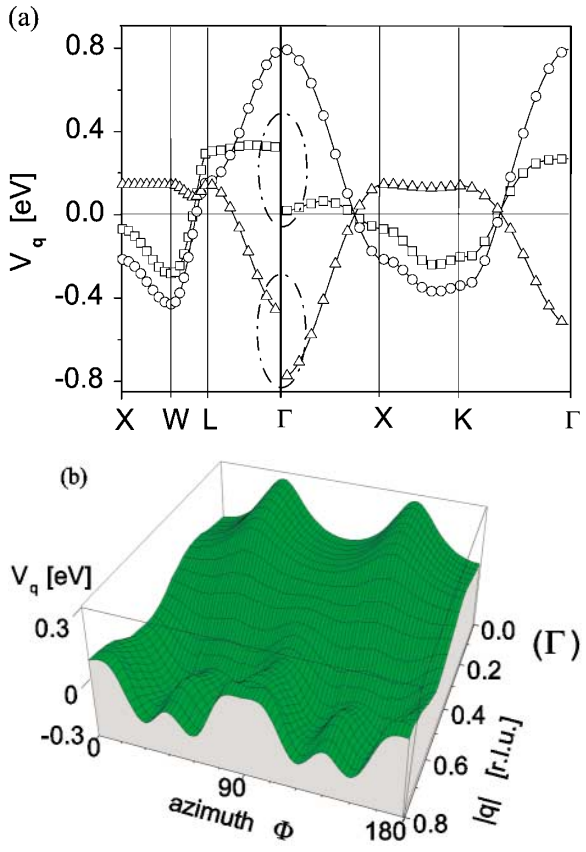

FIG. 2 (color). (a) Calculation of the strain-induced part of the EPI (triangles), the chemical part of the EPI (circles), and the total EPI (squares) along various high-symmetry directions in reciprocal space. The nonanalyticity is marked by ellipses. (b) Polar plot $[(q_x, q_y) \to (q, \Phi)]$ of the EPI in the (100) plane in reciprocal space showing the nonanalyticity at the Γ point. q is given in reciprocal lattice units (r.l.u.).

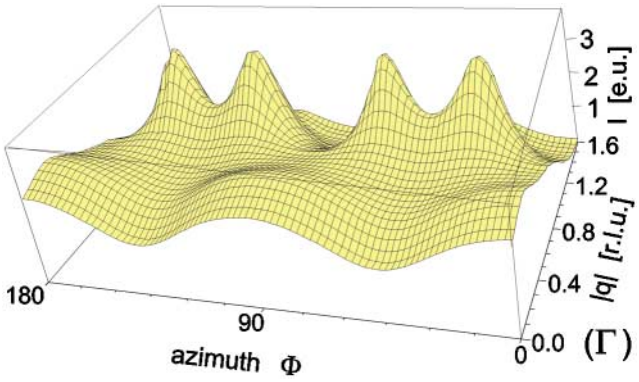

FIG. 3 (color). (a) Polar plot of the calculated diffuse scattering intensity in electron units (e.u.) showing the nonanalyticity at the Γ point. The intensity is calculated for an x-ray energy of 70 keV.

scattering maxima in the vicinity of $(1, 1/2, 0)$ Lifshitz positions. However, an interesting and most unusual feature is predicted at the Γ point. The intensity at $\vec{q} = 0$ exhibits a distinct periodic azimuthal variation which spreads in a wide vicinity of $\vec{q} = 0$. Furthermore, the modulation at the Γ point and around the $(1, 1/2, 0)$ Lifshitz points, where the diffuse scattering has its maximum, are exactly out of phase. Note, also, that this nonanalytic behavior of the diffuse scattering intensity is due to both the distortions $\Phi_{\vec{q}}^2$ and the SRO $\langle |c_{\vec{q}}|^2 \rangle$ in the system.

We have performed a detailed measurement of the diffuse scattering pattern in various high-symmetry planes of $Cu_{83}Mn_{17}$, thereby applying a recently developed ultrafast method for recording diffuse x-ray scattering patterns [20,21]. Using high-energy x-rays ($E = 70$ and 100 keV) at beam lines X17B1 (NSLS, BNL) and BW5 (HASYLAB, DESY) in transmission geometry, we have recorded the diffuse scattering pattern from a 2-mm-thick $Cu_{83}Mn_{17}$ single crystal with various high-symmetry directions aligned parallel to the incident beam. 2D scattering patterns have been recorded *in situ* using both an x-ray CCD camera (MARCCD) and an image plate system (MAR345). Because of the large radius of the Ewald sphere, the deviation of the momentum transfer from the corresponding high-symmetry planes is small close to the center of the image in the first Brillouin zone. During the experiments, the $Cu_{83}Mn_{17}$ sample has been kept in a specially designed vacuum chamber. After annealing the sample at 500 °C for 2 days and at 210 °C for two weeks, the scattering pattern has been recorded at temperature.

Figure 4 shows the center part of the recorded intensity pattern with the (001) surface normal of the sample aligned parallel to the incident beam. Within the first Brillouin zone, the scattering pattern is dominated by diffuse scattering due to SRO and distortions. Inspection of the intensity pattern reveals a clear shift of the diffuse scattering maxima from $(1, 1/2, 0)$ positions. This is due to the distortions present in the system exactly as calculated. Additional features are due to thermal diffuse scattering

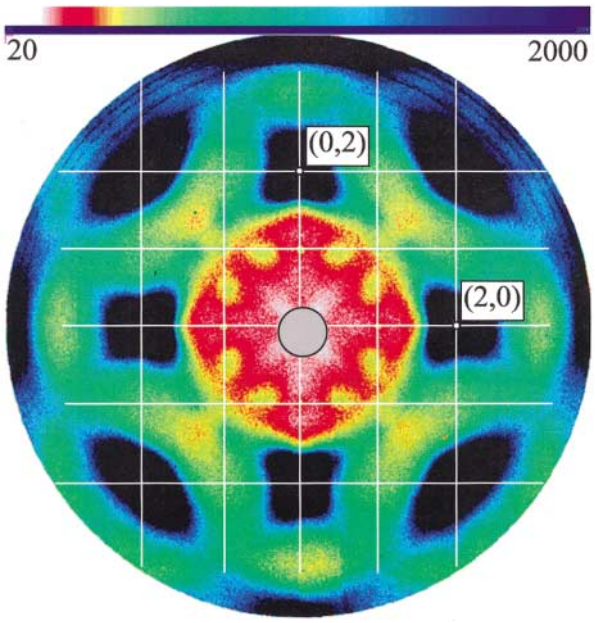

FIG. 4 (color). Measured diffuse intensity pattern with the (001) surface normal oriented parallel to the beam. The center of the image is blocked by the beam stop (grey) shielding the detector from the intense primary beam. The reciprocal lattice is indicated by the white line grid and the color code (inverted) is shown at the top.

which dominates around the positions of the fundamental Bragg reflections. Sharp and weak diffraction features at $(1, 0, 0)$ positions are attributed to a small contamination of the incident beam with higher harmonics ($\lambda/2$).

For a rigorous experimental test of the predicted distortion-induced nonanalytic behavior at the Γ point, we have compared the calculated and experimental diffuse intensity along two azimuthal scans, for $q = 1.1$ reciprocal lattice units (r.l.u.) (scan I in Fig. 5) and for $q = 0.45$ (r.l.u.) closer to the Γ point (scan II in Fig. 5). The diffuse scattering at the Γ point itself is not accessible experimentally. Inspection of Fig. 3 shows, however, that

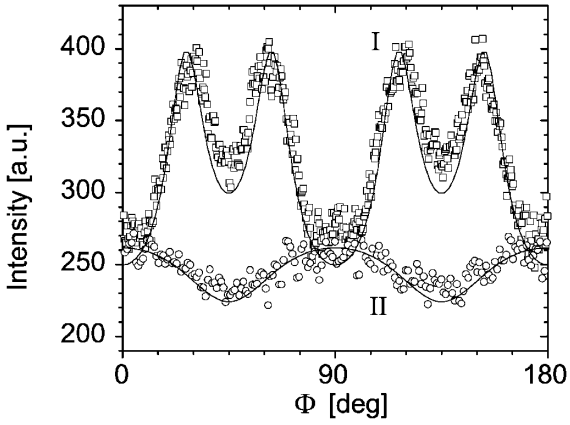

FIG. 5. (a) Azimuthal distribution of the measured (circles and squares) and calculated (lines) diffuse scattering intensity at $q = 0.45$ (r.l.u.) (circles) and $q = 1.1$ (r.l.u.) (squares).

the effects of the Γ point nonanalyticity are visible in a wide vicinity around the Γ point. The striking observation is that the measured intensity modulations for both scans almost exactly reproduce the amplitude and the phase of the calculated diffuse intensities [22]. Notice that scan I (across the Lifshitz points) is most sensitive to $V^{(\mathrm{ch})}$, while scan II is testing a new distortion-induced feature. We want to stress here that in this study the contributions $V^{(\mathrm{ch})}$ and $V^{(\mathrm{si})}$ to the total EPI have been determined separately from diffuse scattering data. The excellent quantitative agreement between the theory and experiment, in particular for the Γ-point modulation (scan II), provides clear evidence for the existence of a distortion-induced nonanalyticity of the SRO intensity at $q = 0$.

In conclusion, our study shows that in ordering alloys the diffuse scattering at and around the Γ point (which has been overlooked thus far) provides essential information about the distortions and the associated energetics in the system. The infinite range of the distortion fields gives rise to a pronounced nonanalytic behavior of the diffuse scattering at the Γ point and to a novel, strongly modulated intensity around it. We have demonstrated this effect theoretically and experimentally in the system $Cu_{83}Mn_{17}$. The detailed analysis of the diffuse scattering by a lattice statics approach revealed that the chemical part of the interaction is rather short ranged and that the long-ranging part is caused entirely by lattice distortions. The significant reduction of free parameters in this model compared to conventional real space models should allow now an extension to systems in confined geometries such as surfaces and thin films.

Research was carried out (in part) at the NSLS, Brookhaven National Laboratory, which is supported by the U.S. Department of Energy, Division of Materials Sciences and Division of Chemical Sciences. We thank J. Hastings, Z. Zhong, and L. Berman (NSLS) for making beam line X17B1 and the CCD-detector available.

[1] M. A. Krivoglaz, *X-Ray and Neutron Diffraction in Nonideal Crystals* (Springer-Verlag, Berlin, 1996); M. A. Krivoglaz, *Diffuse Scattering of X-Rays and Neutrons by Fluctuations* (Springer-Verlag, Berlin, 1996).
[2] J. M. Cowley, J. Appl. Phys. **21**, 24 (1950).
[3] B. E. Warren, *X-Ray Diffraction* (Dover, New York, 1990).
[4] P. C. Clapp and S. C. Moss, Phys. Rev. **142**, 418 (1966); Phys. Rev. **171**, 754 (1968); S. C. Moss and P. C. Clapp, Phys. Rev. **171**, 764 (1966).
[5] A. G. Khachaturyan, *Theory of Structural Transformations in Solids* (Wiley, New York, 1983).
[6] H. Cook and D. de Fontaine, Acta Metall. **17**, 915 (1969).
[7] C. A. Laberge, P. Fratzl, and J. L. Lebowitz, Phys. Rev. Lett. **75**, 4448 (1995); P. Fratzl, O. Penrose, and J. L. Lebowitz, J. Stat. Phys. **95**, 1429 (1999).
[8] S. Dietrich and W. Fenzl, Phys. Rev. B **39**, 8873 (1989).
[9] D. B. Laks, L. G. Ferreira, S. Froyen, and A. Zunger, Phys. Rev. B **46**, 12 587 (1992); V. Ozoliņš and A. Zunger, Phys. Rev. B **57**, 6427 (1998).
[10] M. Asta and S. M. Foiles, Phys. Rev. B **53**, 2389 (1996).
[11] M. Fährmann *et al.,* Acta Metall. Mater. **43**, 1007 (1995).
[12] W. Schweika, *Disordered Alloys,* Springer Tracts in Modern Physics (Springer-Verlag, Berlin, 1998), Vol. 141; B. Schönfeld, Prog. Mater. Sci. **44**, 435 (1999); G. E. Ice and C. J. Sparks, Annu. Rev. Mater. Sci. **29**, 25 (1999).
[13] H. Roelofs, B. Schönfeld, G. Kostorz, and W. Bührer, Phys. Status Solidi (b) **187**, 31 (1995).
[14] B. Schönfeld, O. Paris, G. Kostorz, and J. Skov Pedersen, J. Phys. Condens. Matter **10**, 8395 (1998); H. Roelofs *et al.,* Scr. Mater. **34**, 1393 (1996).
[15] J. W. Cable *et al.,* Phys. Rev. B **29**, 1268 (1984).
[16] M. Hirabayashi *et al.,* J. Phys. Soc. Jpn. **55**, 1591 (1978).
[17] P. Wells and J. H. Smith, J. Phys. F **1**, 763 (1971).
[18] For a parametrization, we used O. P. Gupta, J. Phys. F **14**, 2899 (1984).
[19] R. V. Chepulskii and V. N. Bugaev, J. Phys. Condens. Matter **10**, 8771 (1998).
[20] A. Gibaud *et al.,* J. Appl. Phys. **30**, 16 (1997).
[21] J. Hastings, Z. Zhong, and H. Reichert (to be published).
[22] The thermal diffuse scattering is small within the first Brillouin zone. We have verified that it does not affect our observations.